Received: 30 July 2018 | Revised: 29 August 2018 | Accepted: 31 August 2018

DOI: 10.1002/hbm.24393

WILEY

RESEARCH ARTICLE

Changes in EEG multiscale entropy and power-law frequency scaling during the human sleep cycle

Vladimir Miskovic[1,2] | Kevin J. MacDonald[3] | L. Jack Rhodes[1] | Kimberly A. Cote[3]

[1]Department of Psychology, State University of New York at Binghamton, Binghamton, New York

[2]Center for Affective Science, State University of New York at Binghamton, Binghamton, New York

[3]Psychology Department, Brock University, St Catharines, Ontario, Canada

Correspondence
Vladimir Miskovic, Department of Psychology, State University of New York at Binghamton, 4400 Vestal Parkway East, Clearview Hall, Binghamton, 13902, NY.
Email: miskovic@binghamton.edu

Funding information
Natural Science and Engineering Research Council of Canada

We explored changes in multiscale brain signal complexity and power-law scaling exponents of electroencephalogram (EEG) frequency spectra across several distinct global states of consciousness induced in the natural physiological context of the human sleep cycle. We specifically aimed to link EEG complexity to a statistically unified representation of the neural power spectrum. Further, by utilizing surrogate-based tests of nonlinearity we also examined whether any of the sleep stage-dependent changes in entropy were separable from the linear stochastic effects contained in the power spectrum. Our results indicate that changes of brain signal entropy throughout the sleep cycle are strongly time-scale dependent. Slow wave sleep was characterized by reduced entropy at short time scales and increased entropy at long time scales. Temporal signal complexity (at short time scales) and the slope of EEG power spectra appear, to a large extent, to capture a common phenomenon of neuronal noise, putatively reflecting cortical balance between excitation and inhibition. Nonlinear dynamical properties of brain signals accounted for a smaller portion of entropy changes, especially in stage 2 sleep.

1 | CHANGES IN EEG MULTISCALE ENTROPY AND POWER-LAW FREQUENCY SCALING DURING THE HUMAN SLEEP CYCLE

One of the defining features of consciousness is that it undergoes spontaneous transitions over the course of a day, ranging from wakefulness through varying depths of sleep that encompass synchronous slow-wave episodes interspersed with periods of rapid eye movement (REM) sleep (Llinás & Paré, 1991; Steriade, Timofeev, & Grenier, 2001). These transitions are examples of large-scale self-organized events that reflect delicately tuned competitive interactions between discrete brainstem and basal forebrain nuclei (Brown, Basheer, McKenna, Strecker, & McCarley, 2012; Schwartz & Roth, 2008). The resulting shifts in global states of consciousness are accompanied by widespread changes in the frequency and amplitude of mass cortical electrophysiology. Sleep staging has conventionally been quantified using electroencephalographic (EEG) measures of power in specific frequency bandwidths and the spread of spatially synchronous waves of activity (Pivik, 2007). Another window on the dynamic cortical signatures of sleep and wakefulness is offered by a growing family of non-linear measures related to the temporal complexity of brain signals (see Ma, Shi, Peng, & Yang, 2017 for a review). In spite of the increasing enthusiasm that such measures have garnered recently, it remains unclear how changes in brain signal complexity relate to classical measures of spectral power or what aspect of neurophysiology they reflect. Our aim here was to use distinct sleep stages as a natural physiological context for examining changes in scalp EEG complexity and to relate this to a unified statistical representation of the power spectrum that grounds both phenomena in emerging perspectives on large-scale cortical function.

Functional brain networks are fluidly assembled and disassembled throughout the course of the sleep–wake cycle (Atasoy, Deco, Kringelbach, & Pearson, 2018; Deco, Jirsa, & McIntosh, 2011; Hansen, Battaglia, Spiegler, Deco, & Jirsa, 2015; Tagliazucchi, 2017; Tagliazucchi, Behrens, & Laufs, 2013; Tononi & Koch, 2008). To capture the repertoire of functional networks that form and fragment over time, in terms of the diversity of patterns present in brain signals, researchers have turned to a quantitative metric of uncertainty/complexity known as entropy (Courtiol et al., 2016; Peng, Costa, & Goldberger, 2009; Vakorin & McIntosh, 2012). Entropy denotes the irregularity of time series data—patterns with low predictability are assigned high entropy, while highly ordered, regular signals (e.g., sine waves with fixed frequency) contain very little entropy. When regularity is computed at multiple time scales, it offers one quantitative index of a system's degree of complexity (Costa, Goldberger, & Peng, 2005; Goldberger, Peng, & Lipsitz, 2002; Pincus & Goldberger, 1994).

Accumulating evidence suggests that brain signal entropy tracks gradations in global consciousness. The overall trend reported by studies encompassing human and non-human animal models, is that signal diversity decreases from wakefulness to the NREM-1 and NREM-2 stages, reaching its nadir in slow-wave sleep (SWS), before recovering to near waking levels during REM epochs (Abásolo, Simons, Morgado da Silva, Tononi, & Vyazovskiy, 2015; Acharya, Faust, Kannathal, Chua, & Laxminarayan, 2005; Bruce, Bruce, & Vennelaganti, 2009; Burioka et al., 2005; Lee, Fattinger, Mouthon, Noirhomme, & Huber, 2013; Mateos, Guevara Erra, Wennberg, & Perez Velazquez, 2018; Nicolaou & Georgiou, 2011; Shi, Shang, Ma, Sun, & Yeh, 2017). Convergent findings point to reductions of neurophysiological signal complexity during the loss of consciousness induced by anesthesia (e.g., Ferenets, Vanluchene, Lipping, Heyse, & Struys, 2007; Schartner et al., 2015; Zhang, Roy, & Jensen, 2001) while hallucinogenic drugs produce a diversification of neuronal time series patterns consistent with their profound perceptual, cognitive, and emotional effects (e.g., Schartner, Carhart-Harris, Barrett, & Seth, 2017; Tagliazucchi, Carhart-Harris, Leech, Nutt, & Chialvo, 2014; Viol, Palhano-Fontes, Onias, de Araujo, & Viswanathan, 2017). These findings have paved the way for a novel view of conscious states referred to as the entropic brain theory (Carhart-Harris, 2018; Carhart-Harris et al., 2014), according to which qualitative shifts in mental states can be directly linked to the degree of irregularity evident in macroscopic recordings of neuronal activity. The possibility of having information theoretic based measures of consciousness, accessible from non-invasive EEG recordings, could be further leveraged to investigate a range of sleep disorders, in addition to typical, diurnal variations of the sleep–wake cycle (Ma et al., 2017).

Despite converging findings that the entropy of brain signals changes across distinct conscious states, there are still numerous unresolved theoretical and methodological issues, which limit interpretations of temporal complexity in terms of large-scale cortical events. A major gap stems from the scarce evidence about the degree to which entropy effects are driven by: (i) the linear properties of brain signals (reflected in the power spectrum), (ii) nonlinear time dependencies, or (iii) some combination of the two. The amount of irregularity in time series patterns reflects linear stochastic effects as well as nonlinear deterministic correlations (Courtiol et al., 2016; Kaffashi, Foglyano, Wilson, & Loparo, 2008; Park, Kim, Kim, & Cichocki, 2007; Wang, McIntosh, Kovacevic, Karachalios, & Protzner, 2016). One sleep study that directly explored this question found that single scale estimates of EEG entropy were strongly predicted by the log-transformed ratio of high (alpha and beta) to low frequency (delta and theta) spectral power (Bruce, Bruce, & Vennelaganti, 2009). The authors concluded that high frequency spectral components were entropy raising and lower frequencies entropy suppressing (see also Lee et al., 2013; Mizuno et al., 2010), and that overall, entropy reflects the balance between sleep and alertness promoting factors. The implication here is that entropy changes stem almost entirely from the linear properties of brain signals. Surrogate data analyses, which involve preserving the linear properties of neural time series while simultaneously altering the underlying temporal dependencies via phase randomization, provide a more explicit test for the presence of nonlinearities (Theiler, Eubank, Longtin, Galdrikian, & Farmer, 1992), yet they have not been used frequently (for an exception, see Schartner, Pigorini, et al., 2017).

An intriguing possibility, that we set out to test here, is that sleep-dependent changes in signal complexity and the power spectrum index a common phenomenon of neuronal noise that is driven by state shifts in cortical excitation and inhibition (Waschke, Wöstmann, & Obleser, 2017). Recent work demonstrates that specific features of the broadband power spectrum of neural field recordings (Gao, 2016; Gao, Peterson, & Voytek, 2017; Lombardi, Herrmann, & de Arcangelis, 2017) may be used to make inferences about synaptic excitatory-inhibitory (E:I) balance. It is well established that, within specific ranges, the background frequency spectra of electrophysiological mass activities, including local field potentials, intracranial recordings, and scalp EEG, follow a power-law distribution such that power is inversely proportional to frequency ($1/f$) with a scaling exponent, χ, somewhere between -4 and -1 (Deghani, Bédard, Cash, Halgren, & Destexhe, 2010; Fransson et al., 2013; Freeman, Holmes, Burke, & Vanhatalo, 2003; Freeman & Zhai, 2009; He, 2014; He, Zempel, Snyder, & Raichle, 2010; Podvalny et al., 2015; Pritchard, 1992; Wen & Liu, 2016). Power-law scaling exponents are typically estimated from the slope of a linear fit of the power spectral density (PSD) in log–log coordinates. In terms of a neurophysiological mechanism, PSD slope varies with the strength of temporally correlated population spiking activity, being steeper when neural activity is more synchronized (Freeman & Zhai, 2009; Pozzorini, Naud, Mensi, & Gerstner, 2013; Wen & Liu, 2016). A flatter slope, by contrast, appears to indicate higher background activation (He et al., 2010; Manning, Jacobs, Fried, & Kahana, 2009; Miller et al., 2014; Podvalny et al., 2015) and greater neural noise resulting from neural decorrelation (Gao, 2016; Voytek & Knight, 2015; Voytek et al., 2015).

A computational model that incorporated the differential time constants of glutamatergic (AMPA) and GABAergic synaptic currents found that a reduction in the E:I ratio led to more negatively sloped PSDs, while an increased ratio was associated with slope flattening (Gao et al., 2017; but see Lombardi et al., 2017). Corroborating evidence comes from the observation that the PSD becomes more negatively sloped in electrocorticographic (ECoG) recordings of rhesus monkeys undergoing propofol-induced sedation (Gao et al., 2017). Furthermore, scalp EEG recordings evidence flatter PSD slopes in old relative to young human populations (Voytek et al., 2015), consistent with age-dependent reductions of cortical GABA concentrations in human and non-human primates (He, Koo, & Killiany, 2016; Porges et al., 2017).

Although E:I balance appears to be regulated narrowly across the sleep–wake cycle (Deghani et al., 2010), there is evidence from rodents that glutamate AMPA receptor levels are high in wakefulness and low during sleep (Vyazovskiy, Cirelli, Pfister-Genskow, Faraguna, & Tononi, 2008). In vivo glutamate concentrations are increased during wakefulness and REM sleep, but decreased in NREM sleep of rats (Dash, Douglas, Vyazovskiy, Cirelli, & Tononi, 2009). Echoing these animal studies, magnetic resonance spectroscopy imaging has documented overnight reductions in glutamate + glutamine concentrations within the cortex of healthy human adults, with EEG slow-wave activity being correlated to diurnal glutamate levels (Volk, Jaramillo, Merki, O'Gorman Tuura, & Huber, in press). Concordant with these

observations, neural field models also suggest that states of diminished consciousness are associated with reduced E:I ratios, a collapse in the repertoire of neuronal configurations and a temporal slowing of dominant oscillatory frequencies (Atasoy, Deco, Kringelbach, & Pearson, 2018; Atasoy, Donnelly, & Pearson, 2016). With the progressive disengagement from the external environment that seems to attend increasingly deeper stages of sleep (Cote, 2002; Cote, Etienne, & Campbell, 2001), one would predict that changes in PSD slopes and the diversity of neuronal time series patterns are, to a large extent, reflecting a common underlying neurobiological mechanism. Here, we directly linked the temporal complexity of scalp EEG during different stages of the sleep cycle to variation in the power-law scaling of frequency spectra.

Another significant drawback of previous investigations that we attempted to remedy is that the majority of sleep EEG complexity findings have consisted of entropy measurements at a single time scale (Ma et al., 2017). Complexity in biological systems, however, is characterized by variability over many time scales, from fine (approximately <10 ms) to coarse, such as those 50 ms and above (Garrett et al., 2013; Sejdić & Lipsitz, 2013). A proper measure of a system's complexity necessitates iteratively computing signal regularity over multiple time scales, since even uncorrelated, random signals (e.g., white noise) are high in entropy, despite being low in structural complexity (Costa et al., 2005). Findings gathered from M/EEG (Heisz, Gould, & McIntosh, 2015; McIntosh et al., 2014; Mizuno et al., 2010; Vakorin, Lippé, & McIntosh, 2011; Wang et al., 2016) and fMRI imaging (McDonough & Nashiro, 2014), suggest that entropy at fine time scales indexes local brain dynamics that are characterized by the desynchronization of neuronal assemblies while entropy at the coarse scales is driven by long-range integration and global synchronization processes. In one study that examined multiscale entropy during sleep progression in a healthy sample, the typical finding of increased entropy during wakefulness compared with deep sleep was reported only at fine time scales, which contain a mixture of low and high frequency neural networks (Shi et al., 2017). At longer time scales, primarily containing slow frequencies, this trend was reversed, with deep sleep now marked by increased entropy relative to wakefulness, suggesting that sleep-dependent changes in signal diversity are strongly dependent on the spatiotemporal scale being investigated. However, that study contained a limited set of observations from four participants in total.

1.1 | The present study

Our goal was to use sleep as a naturally occurring physiological context for investigating a concerted set of transitions in the global field dynamics of EEG. Specifically, we aimed to examine changes in the amount of multiscale entropy as individuals cycled through conventional sleep stages, while directly linking the estimated entropy of brain signals to state variability in PSD slopes (spectral tilt), a putative index of cortical E:I balance. In light of previous evidence from neural field models (Atasoy et al., 2016, 2018) and neurophysiological recordings (Tononi & Koch, 2008) that progressive disengagement from the external environment during the deeper (slow wave) stages of sleep is accompanied by decreased E:I ratios, we expected that the rotation of the power spectrum would substantially overlap with shifts in entropy, especially at short time scales. In a more exploratory set of analyses, we performed surrogate (phase shuffled) tests to evaluate the contribution of nonlinear dynamical properties to any of the observed shifts in entropy beyond the second order statistics carried in the EEG power spectrum.

2 | METHOD

2.1 | Participants

Thirty-four young adults (22 women) aged 18–30 years (M = 20.63, SD = 2.68) were recruited from the Brock University population to take part in a study investigating sleep and memory. Participants reported normal sleep of approximately 7–9 hr nightly typically between 22:00 and 08:00 and having not worked shift-work in at least 6 months. Participants reported being healthy, medication-free, and without a history of sleep disorder or psychiatric/neurological condition. Participants were asked to abstain from alcohol, caffeine, vigorous exercise, and naps from 24 hr before their participation until the end of the study. Additionally, all participants were right handed and had learned English before age 8. A $50 honorarium or course credit was provided for participation. All study procedures were approved by the host Institutional Review Board.

2.2 | Procedure

After initial screening procedures via telephone interview, participants gave informed consent and attended one overnight session in the laboratory to screen for evidence of sleep disorders using polysomnography and to acclimatize participants to the sleeping environment before the main study. After eligibility was confirmed, participants returned to the laboratory 2–7 days later for the main protocol. The main protocol consisted of laboratory sessions on two consecutive nights, each with a portion of a memory task and an overnight sleep recording. The memory task component of the protocol is not the focus of current investigation, but the complete details and results of the memory task are reported in MacDonald and Cote (2016). Sessions began at 21:00 with the memory task; electrodes for polysomnography were applied at approximately 22:00, and participants were left undisturbed to sleep in a darkened bedroom from 23:00 until 07:00. The second of these two nights of recorded sleep was selected for the current investigation of sleep EEG.

2.3 | Polysomnography

Neuroscan SynAmps2 amplifiers with SCAN 4.5 software (Compumedics Inc., Abbotsford, Australia) was used to record electrophysiology at 1000 Hz filtered DC to 200 Hz with a 60-Hz notch filter. Gold-plated silver electrodes were applied to sites F3, Fz, F4, C3, Cz, C4, P3, Pz, P4, O1, Oz, and O2 to record EEG with an online reference at site Fpz. To identify sleep stages according to standardized criteria (Rechtshaffen & Kales, 1968), additional peripheral electrodes were placed at sites A1 and A2 for re-referencing, a bipolar electrooculography channel was created from electrodes placed to the sides of

each eye (LEOG and REOG), and a bipolar electromyography (EMG) channel was created from two electrodes placed under the chin. NREM stages 3 and 4 were scored collectively as NREM-3 sleep. Segments used for subsequent analyses were selected from wake (immediately after lights out), early stage 2 sleep (EN2; first bout), late stage 2 sleep (LN2; last bout), NREM-3 (first bout), and each period of REM sleep (R1 to R4), according to the following criteria: Segments were primarily selected from the first five continuous minutes of each stage without evidence of stage transitions or visually identified artifact from movement or other sources. If at least 4 min of continuous, artifact-free data were not available within 10 min of the stage onset, multiple smaller segments were selected from the same 10 min window up to a combined maximum of 5 min. This resulted in each participant's data for a given sleep stage consisting of anywhere from one to six segments (minimum duration of a segment = 27 s). For cases in which multiple smaller segments were used, outcomes variables for each of these segments were averaged together. The LN2 segments were selected with the same criteria except by working from the end of the last NREM-2 bout rather than the start. Since preliminary analyses indicated no reliable difference between EN2 and LN2 or between the successive REM phases, these were subsequently averaged together into a common NREM-2 and REM phase. Supporting Information Table S1 describes the total EEG signal duration by subject and sleep stage.

2.4 | EEG data reduction and analysis

Offline processing of EEG data was accomplished using a combination of EEGLAB (Delorme & Makeig, 2004) functions (for re-referencing and bandpass filtering) and in-house MATLAB routines. After re-referencing the EEG data to Cz, a two-way least squares finite impulse response filter was used to bandpass the time domain signal (high-pass cut-off: 0.1, low-pass cut-off: 50 Hz). Next, peripheral channels A1, A2, REOG, LEOG, and EMG were removed. The remaining frontal (F3, Fz, F4), central (C3, C4), parietal (P3, Pz, P4), and occipital (O1, Oz, and O2) channels were used in subsequent processing and analyses.

2.4.1 | Power spectrum density analyses

The artifact-free time domain data from each electrode were submitted to power spectrum density (PSD) analyses using a modified version of the Welch periodogram method (Tröbs & Heinzel, 2006) with Hanning tapered windows of 2,000 data points (2 s) and 50% overlap. Power spectral density (μV^2/Hz) was estimated for a continuous range from 0.5 to 35 Hz, in 50 logarithmically spaced frequencies. Frequencies less than 0.5 Hz were not included in order to avoid potential slow artifacts arising from skin potentials (e.g., sweating). Frequencies greater than 35 Hz were excluded as there was little power spectral density beyond 30 Hz and we wished to avoid contamination from myogenic sources. Subsequently, frequency spectra were transformed to log–log coordinates in order to calculate the power-law frequency scaling exponent (slope of the line of best for frequencies between 0.5 and 35 Hz) which was estimated using robust linear regression (MATLAB robustfit.m). Frequency bins between 13.5 and 14.7 Hz were omitted from the main analyses presented in the Results section to avoid the influence of periodic sleep spindle oscillations. None of the main findings were affected when fits were estimated using the full range of the frequency spectrum.

2.4.2 | Multiscale dispersion entropy analyses

Multiscale dispersion entropy (MDE) was used to quantify the complexity of EEG signals over numerous time scales (Azami, Rostaghi, Abásolo, & Escudero, 2017; Rostaghi & Azami, 2016). Dispersion entropy is related to sample and permutation entropy, but it is more tolerant to the presence of noise in time series signals and has a considerably shorter computation time (Rostaghi & Azami, 2016). The computational complexity of traditional sample entropy, is higher (O[N^2]) relative to dispersion entropy (O[N]), although both methods yield similar results with high test–retest and internal reliabilities when applied to neural time series data (Kuntzelman, Rhodes, Harrington, & Miskovic, 2018). A schematic depicting some of the major steps in the calculation of dispersion entropy is provided in Figure 1, alongside example time series traces from different global states of consciousness. Briefly, dispersion entropy operates by discovering symbolic dynamics (or dispersion patterns) in a time series and then using Shannon entropy to quantify the resulting uncertainty of these patterns. The first step involves mapping each time series sample to one of c classes (with integer indices from 1 to c) using a mapping based on the normal cumulative distribution function (NCDF), with μ and σ of the NCDF set at the mean and standard deviation, respectively, of the original time series. These remained constant across all scale factors, analogous to keeping the tolerance fixed for sample entropy calculations which, for physiological signals, is preferable to recalculating tolerance at each scale factor (Castiglioni, Coruzzi, Bini, Parati, & Faini, 2017). Note that using NCDF for mapping makes this approach non-linear, resulting in a classified signal (see Figure 1b) matching the size of the original. This approach is robust to observational noise while retaining high sensitivity to amplitude differences and can accept adjacent instances of the same class. Next, a window with embedding dimension (m) and time delay (tau) slides along the signal, counting the frequency of each of c^m potential dispersion patterns (Figure 1c). Finally, the probability of each of these dispersion patterns (Figure 1d) is used to calculate the Shannon entropy where the maximum possible value is $\ln(c^m)$, which would result from all possible dispersion patterns having equal probability. The smallest possible theoretical dispersion entropy value obtains when only one dispersion pattern has a probability greater than zero.

Consistent with the multi-scaling procedure introduced by Costa, Goldberger, and Peng (2002), after an entropy measure is calculated on the original time series of length N, for a given scale factor (π), each non-overlapping set of adjacent samples of length π is averaged producing a new time series of length N/π (rounded down; excess samples at the end of a sequence are discarded). This process is repeated until entropy has been calculated for all time scales of interest.

In keeping with established recommendations (Azami et al., 2017; Rostaghi & Azami, 2016), we fixed the value of c at six for all analyses in this article. The scale factor (π) was set to 300 sample points and the time delay (tau) was set to 1, while the number of embedding dimensions (m) was set to 2 as is common in the literature (e.g., Heisz

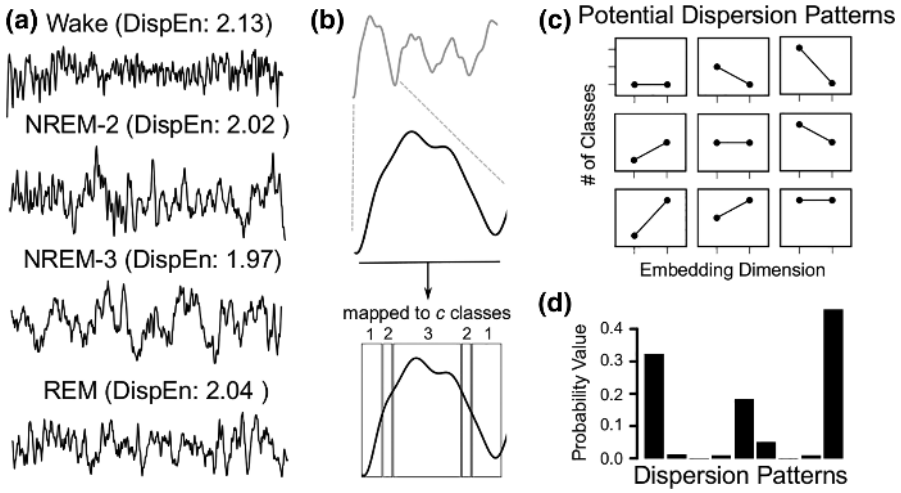

FIGURE 1 (a) Example EEG signal traces (5 s duration) across distinct wake–sleep stages from a randomly selected participant (C4 electrode), along with dispersion entropy estimates from the original time series (i.e., without coarse graining). A schematic depiction of the dispersion entropy calculation process is depicted in (b) starting with a mapping of the original time series signal into a set of *c* classes. For ease of illustration, a mapping to 3 classes is depicted here, which differs from the 6 classes used for actual analyses. In the next step, (c), a set of c^m (for illustration purposes, a total of $3^2 = 9$) symbolic dynamics or dispersion patterns are counted along the length of the entire signal. The relative frequency of each unique dispersion pattern (d) is then tallied and Shannon entropy is calculated on the probability value of all possible dispersion patterns

et al., 2015; McIntosh et al., 2014; Wang et al., 2016). Preliminary analyses were used to ensure the stability of entropy curve differences across a range of free parameter settings. For additional mathematical details on the calculation of dispersion entropy and computational resources, readers are referred to the original publications (Azami et al., 2017; Rostaghi & Azami, 2016).

2.4.3 | Synthetic time series simulations

One way of testing for the contribution of the power spectrum to any entropy related changes would be to attempt to recreate the same pattern of entropy results obtained from empirical EEG recordings using synthetic EEG-like signals. To accomplish this we generated 100 different instantiations of Gaussian white noise sequences (5 min in duration, with a 1 kHz sampling rate). These Gaussian white noise signals were then bandpass filtered using first order Butterworth filters into canonical delta (0.5–4 Hz), theta (4.5–7.5 Hz), alpha (8–13.5 Hz), beta (14–30 Hz), and gamma (30.5–45 Hz) frequency bands. Subsequently, the different bandpass filtered white noise segments were multiplied with weights corresponding to the average spectral density ($\mu V/Hz^2$) in each of the corresponding frequency bands within NREM-3, NREM-2, and REM sleep. Finally, the filtered outputs were summed to create corresponding aggregate signals that would in this way theoretically simulate the power from each of the sleep stages, albeit without the contribution of narrowband sleep spindle oscillations and with random phase coefficients drawn from a uniform distribution between 0 and 2π.

2.4.4 | Surrogate controls

In order to determine whether the differences in entropy between sleep stages could be explained by PSD rotations alone, we conducted a second set of MDE analyses using phase-shuffled surrogate time series signals. The rationale for use of the surrogates is the following: linear processes are completely accounted for by the second order statistics (power spectrum) of a time series. The power spectrum, however, does not contain phase information. The surrogate signals are generated by keeping the power spectrum constant, while randomly shuffling phase (which destroys higher-order correlations) and in the final step, performing an inverse Fourier transform back into the time domain (Theiler et al., 1992). The algorithm that we used to construct the surrogates was the iterated amplitude adjusted Fourier transform (IAAFT) which minimizes the spurious detection of nonlinearity (Schreiber & Schmitz, 1996). Surrogate sets were generated separately for every participant, electrode channel and sleep stage (using a maximum number of 100 iterations) and then, these surrogates were used to construct ratio scores of original relative to surrogate data, similar to what has been reported in other studies (Schartner, Carhart-Harris, et al., 2017; Schartner, Pigorini, et al., 2017). In brief, the normalized ratios were calculated as $MDE_{original}/MDE_{surrogate}$ for each sleep stage. Accordingly, if sleep stage contrast reversed in direction between the original and the surrogate set of analyses (e.g., REM > NREM-3 for the original MDE analyses, but REM < NREM-3 for surrogate normalized ratios), then it can be concluded that the entropy differences are explained entirely by linear processes. In the absence of a direction reversal, the contribution of nonlinearity to the sleep stage differences in entropy can be inferred.

2.5 | Statistical analyses

Since we wished to avoid averaging MDE values across a priori time scale factors and since we had no specific regional electrode hypotheses, we adopted a mass univariate approach to testing for changes in EEG signal complexity. To detect reliable differences in EEG entropy as a function of sleep stage, we submitted the MDE values to a paired samples, two-tailed permutation test based on the t_{max} statistic (Blair & Karniski, 1993; Groppe, Urbach, & Kutas, 2011) using a family-wise alpha level of 0.01, effectively controlling for the inflation

of Type I error rates. All 300 scale factors at 11 cephalic electrodes were included in the test (i.e., 3,300 total comparisons). Adopting a Monte Carlo approach, we used 5,000 random within-participant permutations of the data to empirically approximate the null distribution for the contrasts of interest. Based on this estimate, critical *t*-scores were derived and any differences in the original data that exceeded the t_{max} statistic were deemed reliable.

To test for differences in $PSD^{0.5–35\ Hz}$ slopes, we conducted repeated-measures ANOVAs using the within-subject factors of Sleep Stage (NREM-3, NREM-2, and REM) and Region (frontal, central, parietal, and occipital). All ANOVA models were evaluated using Type III Sums of Squares and Greenhouse–Geisser corrections were applied in cases where Mauchly's test revealed violations of the sphericity assumption.

All statistical analyses were performed using a combination of functions from MATLAB and R (R Development Core Team, 2008).

3 | RESULTS

3.1 | Multiscale entropy across sleep stages

Figure 2 depicts thresholded (p_{perm} < .01) maps of the mass univariate contrasts between successive sleep stages. As a general pattern, multiscale entropy followed the pattern of REM > NREM-2 > NREM-3, for time scales up to approximately 100 ms. At temporal scales larger than approximately 100 ms, entropy estimates are largely based on frequencies in the theta and delta bandwidths. When contrasting NREM-2 relative to the NREM-3 stage, entropy was higher in the former up to a temporal scale factor of approximately 70 ms and then reversed in direction from a scale factor of approximately 110 ms up to 300 ms across all electrode locations (Figure 2, *left panel*). A similar pattern obtained for the REM to NREM-3 contrast, except that the enhanced entropy in the former stage persisted until a scale factor of approximately 100 ms (at least at the posterior electrodes) and did not reverse in direction until after approximately 150 ms (see Figure 2, *middle panel*). Relative to NREM-2, there was more entropy during REM sleep up to a temporal scale of approximately 150 ms (Figure 2, *right panel*), at least at the posterior electrodes as well as at the frontal midline (Fz).

3.2 | $PSD^{0.5–35\ Hz}$ slopes across sleep stages

The results of the repeated measures ANOVA revealed main effects of Sleep Stage, $F(2,66) = 607.53$, Greenhouse–Geisser corrected $p < 3.13 \times 10^{-43}$, $\eta^2_p = .87$, and Region, $F(3,99) = 109.95$, Greenhouse–Geisser corrected $p = 3.50 \times 10^{-23}$, $\eta^2_p = .16$. As shown in Figures 3 and 4, PSDs were increasingly more negatively sloped from REM to NREM-2 to NREM-3 sleep (all pairwise *p*s ≤ .001). It can be seen from inspection of Figure 3 that change in the slow frequency bands (delta and theta bandwidths) across sleep stages was considerably more pronounced than increases in the higher frequencies, so that it can be inferred that slow waves were the major driver of PSD slope shifts depicted in Figure 4 (see Supporting Information Figure S1 for mass univariate contrasts of spectral power across all electrodes and frequency bins).

In terms of the regional distribution of $PSD^{0.5–35\ Hz}$ slopes, the steepest slopes were observed at the frontal electrode cluster ($M = -1.90$, $SD = 0.50$) and the least negatively sloped PSDs obtained at the central cluster ($M = -1.72$, $SD = 0.48$). The frontal and occipital ($M = -1.88$, $SD = 0.45$) electrode clusters did not differ from each other, but all other pairwise regional contrasts reached significance (*p*s < 1×10^{-14}).

3.3 | Linking entropy to $PSD^{0.5–35\ Hz}$ Slopes

Since there were notable individual differences in the distribution of $PSD^{0.5–35\ Hz}$ slopes within each sleep stage, we next examined whether this was related to individual differences in EEG entropy values. Figure 5 shows the Spearman's *rho* correlations between PSD slopes and entropy across the full range of temporal scales for the

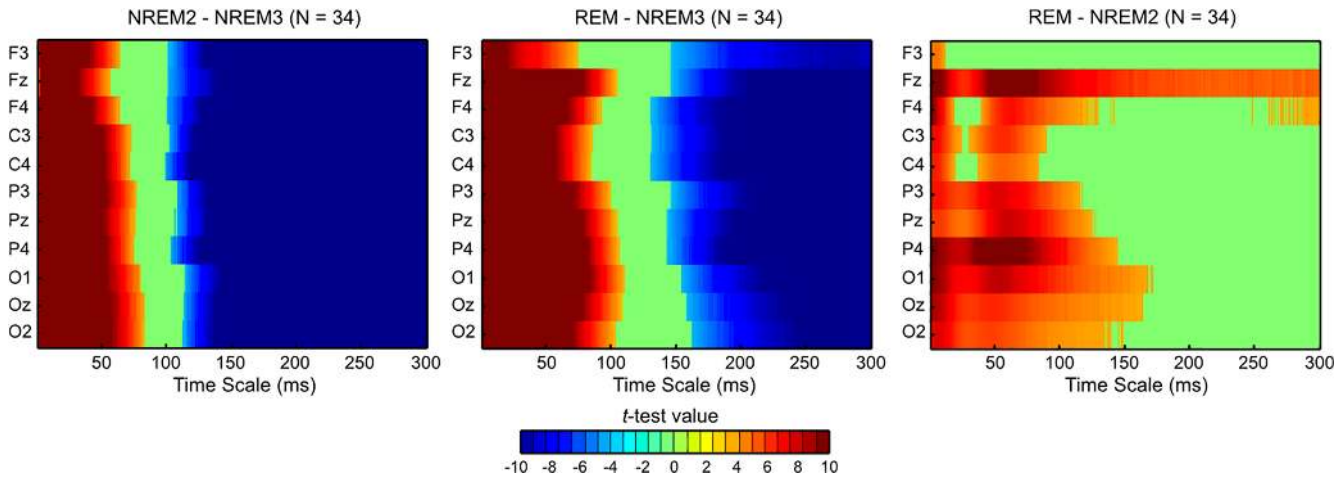

FIGURE 2 Statistical saliency maps depicting mass univariate contrasts of dispersion entropy at each electrode and time scale factor. Colors represent *t*-test values (hot colors indicate higher entropy for the sleep stage indicated first for a given contrast and cool colors indicate the opposite pattern), masked by significance as determined using the t_{max} Monte Carlo method (with 5,000 random within-subject data permutations). Green areas depict contrasts that did not survive statistical thresholding (p_{perm} < .01) [Color figure can be viewed at wileyonlinelibrary.com]

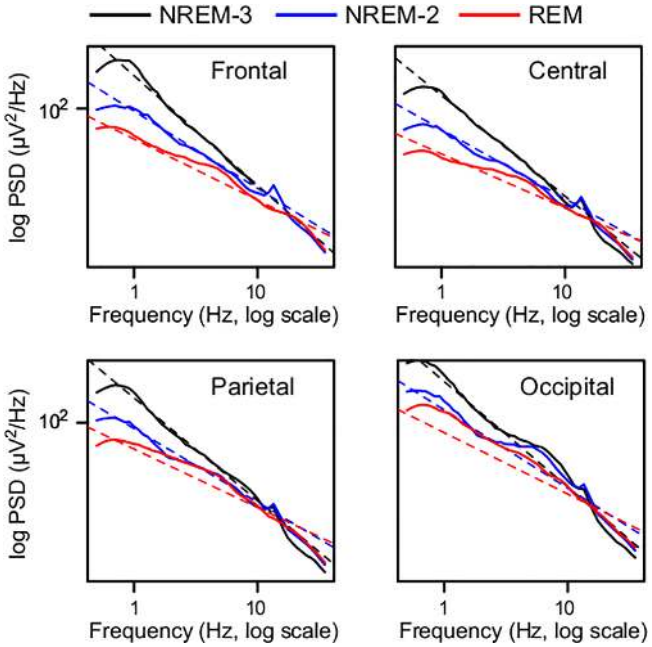

FIGURE 3 Averaged power spectral density (PSD) plots (on a log–log scale) shown separately for each sleep stage and electrode cluster region along with robust fits (dashed lines) [Color figure can be viewed at wileyonlinelibrary.com]

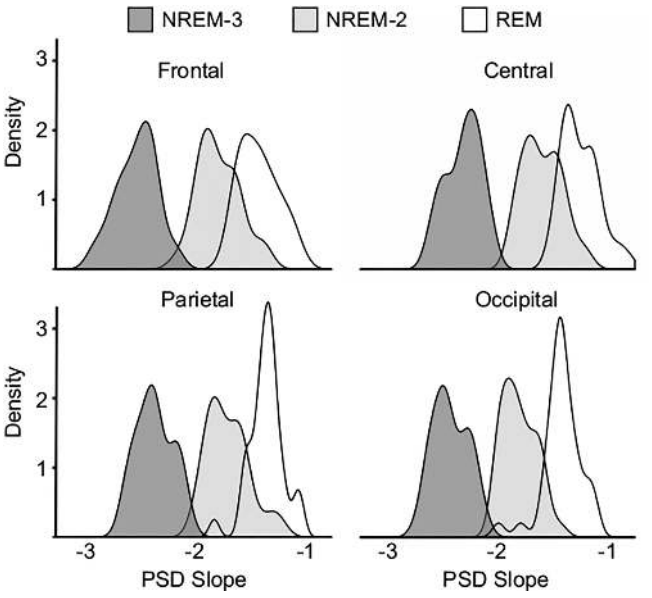

FIGURE 4 Kernel densities for each sleep stage showing the distribution of power-law exponents of EEG spectra (PSD slope) estimated using a robust linear regression

different sleep stages, averaged over EEG electrodes. Higher dispersion entropy at time scales up to approximately 50 ms was predicted by shallower $PSD^{0.5–35\ Hz}$ slopes with increasingly less explained variance at larger scale factors. At coarse time scales of approximately 200–300 ms this relationship reversed (at least during NREM-3 and NREM-2 sleep), such that more negatively sloped PSDs became associated with higher entropy values.

Next, we averaged dispersion entropy at both the fine (1–10 ms) and coarse (250–300 ms) time scales and then calculated difference scores across successive sleep stages. Subsequently, we evaluated linear regression models in which we regressed the stage-dependent changes in dispersion entropy on stage-dependent changes in $PSD^{0.5–35\ Hz}$ slopes. Approximately 59–70% of the variance in fine scale entropy was predicted by variation in the frequency scaling of EEG spectra (see Figure 6a). By contrast, a smaller proportion of coarse entropy variance could be explained by stage-dependent differences in PSD slopes.[1]

3.4 | Synthetic EEG-like signals

To further explore the extent to which the multiscale entropy changes observed above, including the cross-over of entropy values at coarser time scales, were driven by the underlying spectral power changes alone, we next turned to simulations using synthetic EEG-like signals created from linear summations of bandpass filtered Gaussian white noise. As illustrated in Figure 7, the general trend of REM > NREM-2 > NREM-3 entropy at fine time scales was reproduced using these synthetic EEG-like signals, as well as the reversal of this pattern at coarse time scales. However, there were also notable differences between the entropy curves obtained from synthetic signals relative to the scalp EEG epochs (Figure 7b), especially at large time scale factors. In general, the stage-dependent differences in the magnitude of entropy tended to be underestimated in the synthetic data. These differences possibly stem from nonstationary sleep spindle oscillations, which are dominant during NREM-2 and NREM-3 sleep. The contribution of EEG phase dynamics to estimates of brain signal complexity is not captured in signals simulated using band-pass filtered noise.

3.5 | Surrogate normalized multiscale entropy analyses

In order to determine the contribution of nonlinear dependencies to stage-dependent changes in entropy, we conducted another round of mass univariate analyses using EEG signals that were normalized by phase-shuffled IAAFT surrogates.[2] The results of these analyses are depicted in Figure 8. Many of the changes in entropy between NREM-2 and NREM-3 stages remained even after this normalization procedure, providing evidence that the shifts in complexity were not driven entirely by information contained in the power spectrum but also stemmed from higher-order properties of brain signals. Virtually all of the differences in entropy between REM sleep and NREM-3 were eliminated, while a larger proportion of entropy differences between REM and NREM-2 stages, at coarse time scales, survived the surrogate testing procedure.

[1]Predicting stage-dependent changes in fine time scale dispersion entropy from changes in slow-wave power alone (i.e., log transformed delta and theta spectral power density), accounted for 60, 54, and 53% of the variance in ΔNREM2-NREM2, ΔREM-NREM3, and ΔREM-NREM2 shifts respectively (all *p*s < .0001). The increase in slow-wave power from the NREM2 to the NREM3 stage explained 36% of the variance in coarse entropy.

[2]As verification that the normalized entropy scores reduced sensitivity to signal spectral content, we observed reduced and nonsignificant correlations between individual differences in PSD slopes and normalized entropy measures (in contrast to the non-normalized entropy values; see Figure 4).

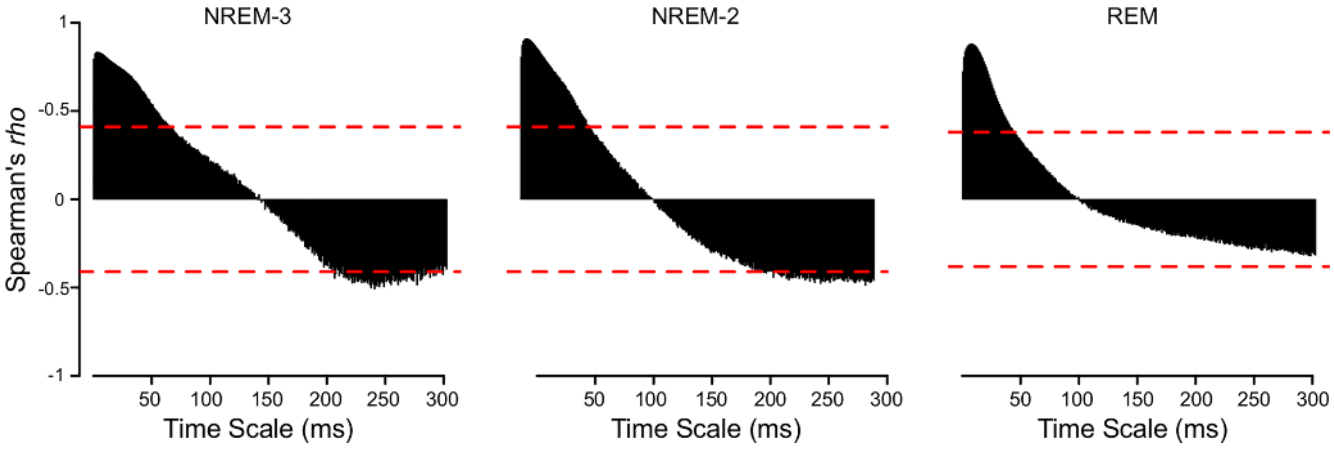

FIGURE 5 Spearman's *rho* correlations (*df* = 33) between the absolute levels of dispersion entropy at scales 1–300 ms and PSD slope. Dashed lines indicate the correlation strengths corresponding to the 99th percentile of *rho* coefficients built from an empirical distribution of 5,000 random data permutations [Color figure can be viewed at wileyonlinelibrary.com]

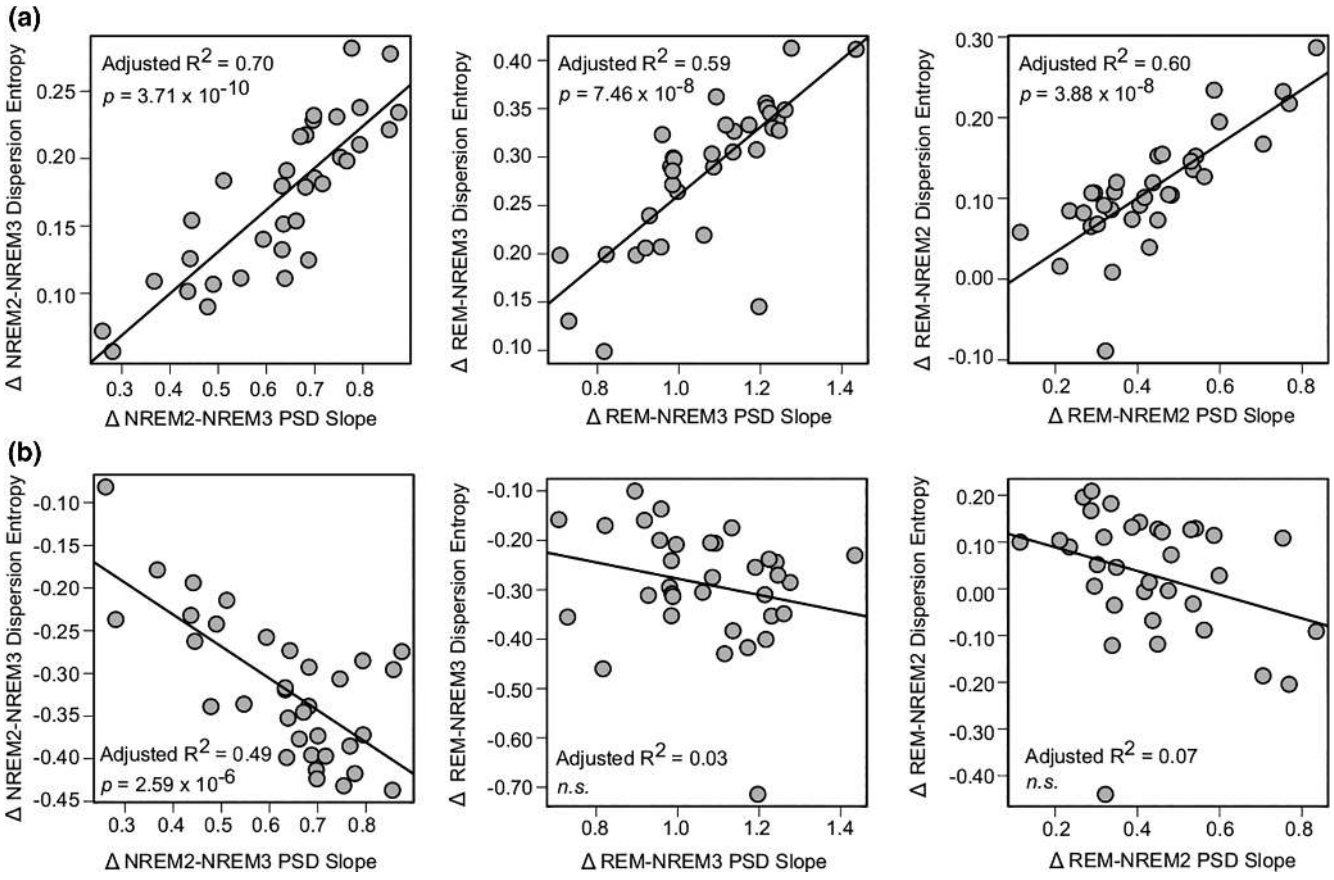

FIGURE 6 Linear models regressing (a) Δ dispersion entropy at the fine (1–10 ms) and (b) coarse (250–300 ms) time scales on Δ PSD slopes, averaged over all electrodes

To test whether the occurrence of spindles during NREM-2 sleep contributed to the degree of entropy during this stage, we calculated Spearman's *rho* correlations between NREM-2 spindle counts (manually counted over the full night at Cz) and dispersion entropy at fine and coarse time scale factors (see Table 1). These analyses revealed a positive association between NREM-2 spindle count and entropy at fine time scales, except at the occipital electrode cluster.

3.6 | REM sleep versus pre-sleep wakefulness

Finally, in a set of follow-up comparisons, we contrasted multiscale entropy and $PSD^{0.5-35\ Hz}$ slopes between REM sleep and pre-sleep wakefulness (immediately after lights out) in a smaller subset of participants (*N* = 30) who had usable wake epochs. As illustrated in Figure 9, wakefulness was associated with higher entropy up to scale factors of approximately 40 ms while REM entropy was greater than

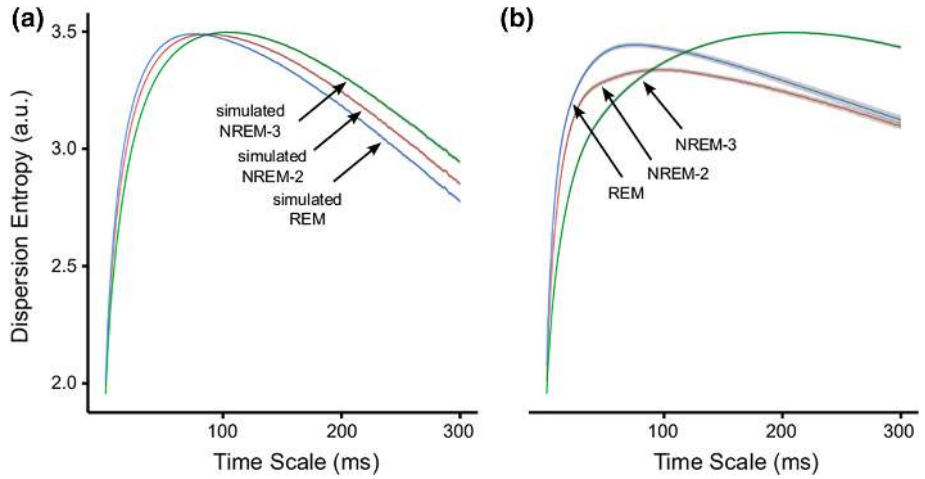

FIGURE 7 Multiscale dispersion entropy curves estimated from (a) bandpass filtered Gaussian white noise samples constructed to have the same theoretical power spectra as NREM-3, NREM-2, and REM sleep respectively (average of 100 simulated signals) or from (b) empirical EEG recordings (average of all electrodes and participants). Shading indicates ±1 *SEM* [Color figure can be viewed at wileyonlinelibrary.com]

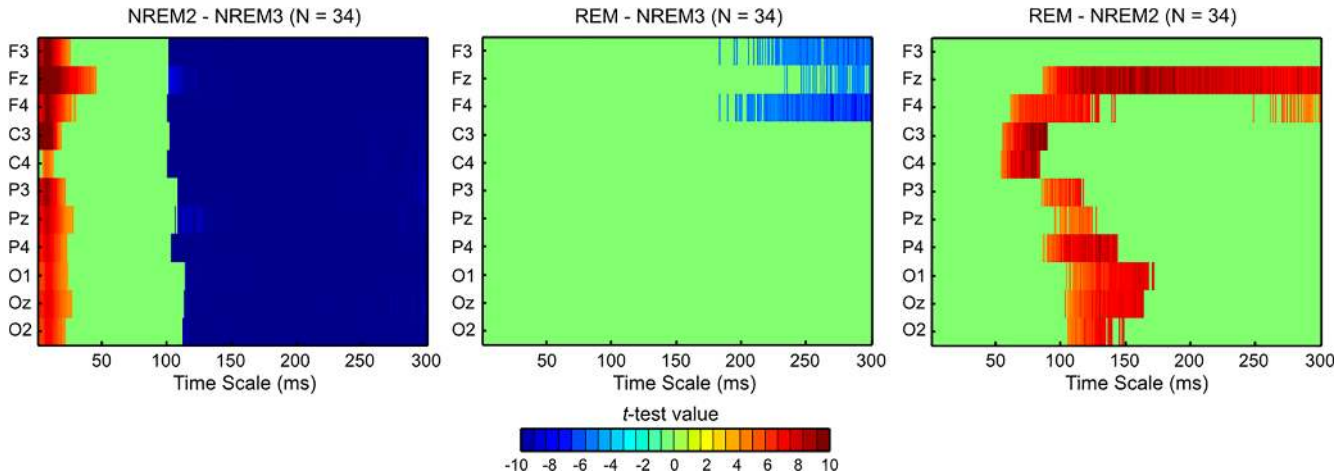

FIGURE 8 Statistical saliency maps depicting mass univariate contrasts of dispersion entropy at each electrode and time scale factor, normalized by IAAFT phase-shuffled surrogates. Colors represent *t*-test values (hot colors indicate higher entropy for the sleep stage indicated first for a given contrast and cool colors indicate the opposite pattern), masked by significance as determined using the t_{max} Monte Carlo method (with 5,000 random within-subject data permutations). Green areas depict contrasts that did not survive statistical thresholding (p_{perm} < .01) [Color figure can be viewed at wileyonlinelibrary.com]

TABLE 1 Spearman's *rho* correlations between NREM-2 spindle count and NREM-2 dispersion entropy

Region	Time scale of entropy	Rho	*p* value
Frontal	1–10 ms	**0.46**	**.01**
	250–300 ms	0.05	.79
Central	1–10 ms	**0.41**	**.02**
	250–300 ms	0.12	.53
Parietal	1–10 ms	**0.39**	**.03**
	250–300 ms	0.13	.48
Occipital	1–10 ms	0.31	.10
	250–300 ms	0.18	.34

during wakefulness from a time scale of approximately 60 ms until 300 ms at the majority of electrodes. None of the differences in entropy between REM sleep and wakefulness remained after using phase shuffled surrogate tests for nonlinearity.

The robust regression estimates of $PSD^{0.5-35\ Hz}$ slopes for the wake segments excluded frequency bins between 9 and 11 Hz containing prominent non-broadband alpha oscillation peaks. These analyses revealed a main effect of global consciousness state, $F(1,29) = 169.64$, $p < 1.21 \times 10^{-13}$, $\eta^2_p = .59$, with more negatively sloped PSDs during REM sleep ($M = -1.36$, $SD = 0.18$) compared with wakefulness ($M = -0.92$, $SD = 0.24$).

4 | DISCUSSION

We explored changes in multiscale brain signal entropy and power-law scaling exponents of EEG frequency spectra across the sleep cycle. Overall, our findings suggest that the changes in entropy that occur throughout the sleep cycle are strongly dependent upon the time scale being investigated. In addition, we discovered that, although a large portion of the stage-specific changes of signal

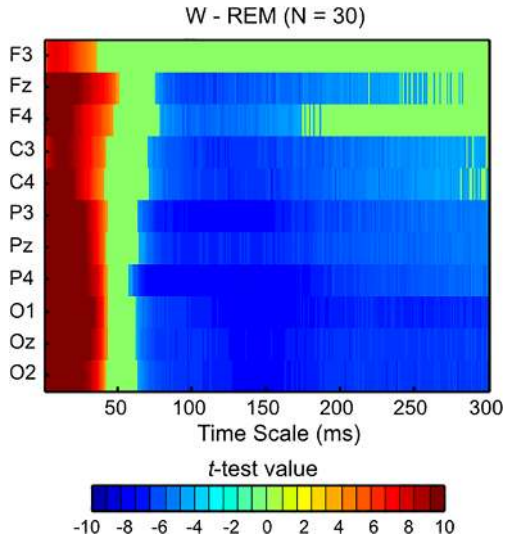

FIGURE 9 Mass univariate contrasts of dispersion entropy at each electrode and time scale factor. Colors represent *t*-test values (hot colors indicate higher entropy in pre-sleep wakefulness relative to REM sleep and cool colors indicate the opposite pattern), masked by significance as determined using the t_{max} Monte Carlo method (with 5,000 random within-subject data permutations). Green areas depict contrasts that did not survive statistical thresholding ($p_{perm} < .01$) [Color figure can be viewed at wileyonlinelibrary.com]

complexity can be seen to overlap with a rotational shift of the EEG power spectrum (spectral tilt), some of the variability is driven by signal phase dynamics, particularly stemming from endogenous events occurring during stage 2 sleep.

4.1 | Entropy at fine time scales

The reduction of brain signal complexity with increasing sleep depth is in good agreement with previous findings in humans (Acharya et al., 2005; Bruce et al., 2009; Burioka et al., 2005; Lee et al., 2013; Nicolaou & Georgiou, 2011; Shi et al., 2017) and rodents (Abásolo et al., 2015). Our results extend this body of knowledge by measuring multiscale brain signal variability in contrast to the majority of previous studies that have quantified entropy/complexity at single time scale factors, without performing temporal coarse graining (except for Shi et al., 2017).

Another way in which our study helps to extend prior work is by explicitly linking the entropy of brain signals to the $1/f^{\chi}$ component of power spectra (see Sheehan, Sreekumar, Inati, & Zaghloul, 2018 and Waschke et al., 2017). The PSD slope of large-scale field potentials has been proposed to be a measure of neural noise that reflects population spiking statistics (Voytek & Knight, 2015; Voytek et al., 2015). Since the degree of entropy at smaller time scales has been hypothesized to measure local information processing within asynchronous neuronal assemblies (Heisz et al., 2015; McDonough & Nashiro, 2014; McIntosh et al., 2014; Mizuno et al., 2010; Vakorin et al., 2011; Wang et al., 2016), our finding of a positive association between fine scale entropy and PSD slopes is to be expected (see also, Waschke, Wöstmann, & Obleser, 2017). If the entropic content of brain signals at fine time scales is intimately linked with variation in the slope of the EEG power spectrum, what might be the common neurophysiological mechanism that underlies this? Combining evidence from computational modeling and cross-scale recordings in nonhuman animal preparations, variation in PSD slopes has been proposed to provide an aggregate read-out of fluctuations in E:I balance (Gao et al., 2017). Our results here can be seen as essentially consistent with this hypothesis in so far as increasing sleep depth is accompanied by greater inhibitory (or reduced excitatory) activity (Atasoy et al., 2018; Tononi & Koch, 2008) and lowered global levels of consciousness (Cote, 2002; Cote et al., 2001). A major caveat here is that the hypothesis that PSD slopes index E:I balance (and exactly how they index it) remains up for debate (Gao, 2016; Gao et al., 2017; Lombardi et al., 2017), especially at the level of extracranially recorded brain signals which do not contain the sensitive high gamma range that is accessible in intracranial recordings (He et al., 2010). Supportive evidence can be gleaned from a recent study, which noted that overnight reductions in cortical glutamate metabolites were positively correlated to scalp-recorded slow-wave activity (Volk et al., in press)—a finding that extends similar results from rodents (Dash et al., 2009). In the future, combined EEG and pharmacology studies would offer a more direct way to test some of tentative interpretations offered here, by examining the effects of agents that modulate the level of inhibition and excitation of cortical neurons. Anesthetic compounds like propofol, whose actions at the level of GABA neurotransmission are well characterized (Concas, Santoro, Serra, Sanna, & Biggio, 1991) and psychedelic drugs that increase cortical excitation (Celada, Puig, & Artigas, 2013) and produce broadband desynchronization of MEG signals (Muthukumaraswamy et al., 2013), might be particularly suitable candidates for further research.

A final point is worth noting here. A previous sleep study (Bruce et al., 2009) has reported that EEG entropy of the original time series was strongly predicted by the logarithmically transformed power ratio of fast to slow frequencies. Our results provide confirmatory evidence but also suggest a slightly different interpretation of those findings, namely that this ratio can be alternatively conceptualized as a flattening of the PSD slope resulting from a rotation of the neurophysiological power spectrum (Voytek & Knight, 2015).

4.2 | Entropy at coarse time scales

The entropic level of NREM-3 sleep was increased relative to NREM-2 and REM at large time scales (see also Shi et al., 2017). This suggests a shift toward more distributed, rather than local, entropy as cortical activity switches into a global bistable pattern of depolarized (up) and hyperpolarized (down) states characteristic of slow-wave sleep (Sanchez-Vives & McCormick, 2000). Findings from a variety of different recording modalities (EEG, MEG and fMRI) have demonstrated that entropy at small time scales (approximately < 10 ms) is inversely correlated, while entropy at coarser time scales (approximately > 50 ms), is positively correlated with long-range brain functional connectivity (McDonough & Nashiro, 2014; McIntosh et al., 2014; Vakorin et al., 2011). It is possible, therefore, that the increased entropy of slow-wave sleep at long time scales originates from the action of distant synchronization processes. Indeed, electrophysiological measures have documented that functional connectivity, within specific band-limited frequencies, particularly in the slow (1–2 Hz)

range tends to be highest in deep NREM sleep (Achermann & Borbély, 1998a,b)—an effect that is independent of signal amplitude (Achermann & Borbély, 1998b; Nayak et al., 2017). Cortical hypersynchrony has also been demonstrated to alter the routing of information and predict diminution of consciousness during sedation (Supp, Siegel, Hipp, & Engel, 2011).

On the surface, the evidence just reviewed may seem to be contradicted by studies reporting a breakdown of effective connectivity (Massimi et al., 2005) and fMRI functional connectivity (e.g., Spoormaker et al., 2010) during NREM sleep. Clearly any broad statements concerning global hyper- or hypo-connectivity associated with a given mental state are bound to be oversimplifications without taking into account spatiotemporal scale dependency that is inherent in neural time series data or the differences in recording modalities. Moreover, there is a large heterogeneity of mental state-dependent changes depending on the constituent modular network that is under investigation and whether one is measuring total, between or within-system integration (e.g., Boly et al., 2012; Tagliazucchi, von Wegner, et al., 2013). Unfortunately, this level of detail is not accessible in the sparse recording montage employed in our study. However, a more general interpretation of the scale-dependent crossover of entropy observed here suggests that the mix between functional integration and segregation that determines the complexity of a system's output (Pedersen, Omidvarnia, Walz, Zalesky, & Jackson, 2017) is tipped in favor of integration at the distributed level during deep NREM sleep and in favor of local integration during REM sleep and waking.

4.3 | Nonlinear contributions

The high amounts of variance in EEG entropy explained by variation in $PSD^{0.5-35\ Hz}$ slopes—between 60 and 70% at fine time scales and approximately 40% at coarse scales—indicates that a substantial portion of the state-dependent changes in scalp EEG complexity is driven by linear stochastic effects (see also Pereda, Gamundi, Rial, & González, 1998 and Shen, Olbrich, Achermann, & Meier, 2003 for additional evidence of weak nonlinearity in human sleep EEG). However, higher-order dynamical properties of brain activity also accounted for some of the stage-dependent complexity changes (see also Schartner, Carhart-Harris, et al., 2017; Schartner, Pigorini, et al., 2017). This conclusion can be drawn from two separate lines of evidence. First, the multiscale entropy curves of bandpass filtered noise with the same theoretical power spectra as NREM-3, NREM-2, and REM sleep, while reproducing many of the effects obtained in EEG data, also seemed to underestimate the state differences in signal complexity suggesting that phase spectra contribute to some of the entropy changes. Second, the results of our phase-shuffled IAAT surrogate normalized entropy analyses confirm that nonlinear dependencies additionally contribute to some of the differences in entropy between NREM-2 and REM as well as between NREM-2 and NREM-3 sleep. By contrast, virtually all of the differences in entropy between NREM-3 and REM as well as between REM and waking appear to be explained by EEG power. Our findings underscore recent recommendations (Courtiol et al., 2016) that analyses of brain signal complexity should include the combined examination classical spectral power effects as well as the use of surrogate time series in order to guide proper interpretation—a feature that has been largely lacking in prior literature on EEG entropy changes during sleep.

On the whole, nonlinear dynamics exerted a stronger influence at coarser time scales relative to smaller ones that were the focus in previous sleep EEG studies (e.g., Bruce et al., 2009). This is consistent with evidence that coarse graining alleviates the linear stochastic effects in time series signals (Kaffashi et al., 2008; Vakorin & McIntosh, 2012). The presence of nonlinearities during the NREM-2 stage in particular, appears to be in line with prior findings (Shen et al., 2003) where this was attributed to the presence of sleep spindles and K-complexes. This hypothesis was partially supported by our finding of a positive correlation between NREM-2 spindle count and the degree of EEG signal entropy, highlighting a role for phase-dependent signal characteristics.

5 | CONCLUSIONS

In sum, we found that changes in the entropy of global field EEG dynamics throughout the sleep cycle are strongly time-scale dependent. At shorter time scales, that putatively measure local information processing in brain networks, entropy followed a pattern of REM > NREM-2 > NREM-3 (with the greatest entropy observed during pre-sleep wakefulness). At longer time-scales, this pattern reversed, resulting in the greatest amounts of distributed entropy during the deepest stage of sleep (NREM-3). To a large extent, this time-scale dependent cross-over of entropy could be explained by the linear stochastic effects of the power spectrum, with a slower time constant during NREM-3 sleep. Critically, temporal signal complexity (at small time scales) and the slope of EEG power spectra appear to be largely overlapping representations of neuronal noise. Additionally, some of the changes in EEG complexity across the human sleep cycle cannot be explained by linear dependencies alone but are also driven by phase dynamics. It can be speculated that neuronal events occurring during the NREM-2 stage, in particular, are important contributors to estimates of brain signal complexity. Our findings raise the possibility that, in the future, the joint investigation of EEG power-law frequency scaling and signal entropy measures, which reflect both shared and unique aspects of neural signal complexity (Sheehan et al., 2018), could assist in understanding changing consciousness levels, sleep regulation and disruptions to sleep mechanisms in a variety of sleep disorders.

ACKNOWLEDGMENTS

Data was collected in the Brock University Sleep Research Laboratory which is funded by the Natural Science and Engineering Research Council (NSERC) of Canada. The funding agency had no role in the analysis and interpretation of the data or in the writing of this manuscript.

CONFLICT OF INTEREST

The authors declare that they have no conflicts of interest

ORCID

Vladimir Miskovic https://orcid.org/0000-0001-6440-5347

REFERENCES

Abásolo, D., Simons, S., Morgado da Silva, R., Tononi, G., & Vyazovskiy, V. V. (2015). Lempel-Ziv complexity of cortical activitiy during sleep and waking in rats. *Journal of Neurophysiology*, *113*, 2742–2752.

Acharya, U. R., Faust, O., Kannathal, N., Chua, T., & Laxminarayan, S. (2005). Non-linear analysis of EEG signals at various sleep stages. *Computer Methods and Programs in Biomedicine*, *80*, 37–45.

Achermann, P., & Borbély, A. A. (1998a). Coherence analysis of the human sleep electroencephalogram. *Neuroscience*, *85*, 1195–1208.

Achermann, P., & Borbély, A. A. (1998b). Temporal evolution of coherence and power in the human sleep electroencephalogram. *Journal of Sleep Research*, *7*, 36–41.

Atasoy, S., Deco, G., Kringelbach, M. L., & Pearson, J. (2018). Harmonic brain modes: A unifying framework for linking space and time in brain dynamics. *The Neuroscientist*, *24*, 277–293.

Atasoy, S., Donnelly, I., & Pearson, J. (2016). Human brain networks function in connectome-specific harmonic waves. *Nature Communications*, *7*, 10340.

Azami, H., Rostaghi, M., Abásolo, D., & Escudero, J. (2017). Refined composite multiscale dispersion entropy and its application to biomedical signals. *IEEE Transactions on Biomedical Engineering*, *64*, 2872–2879.

Blair, R. C., & Karniski, W. (1993). An alternative method for significance testing of waveform difference potentials. *Psychophysiology*, *30*, 518–524.

Boly, M., Perlbarg, V., Marrelec, G., Schabus, M., Laureys, S., Doyon, J., … Benali, H. (2012). Hierarchical clustering of brain activity during human nonrapid eye movement sleep. *Proceedings of the National Academy of Sciences of the United States of America*, *109*, 5856–5861.

Brown, R. E., Basheer, R., McKenna, J. T., Strecker, R. E., & McCarley, R. W. (2012). Control of sleep and wakefulness. *Physiological Reviews*, *92*, 1087–1187.

Bruce, E. N., Bruce, M. C., & Vennelaganti, S. (2009). Sample entropy tracks changes in electroencephalogram power spectrum with sleep state and aging. *Journal of Clinical Neurophysiology*, *26*, 257–266.

Burioka, N., Miyata, M., Cornélissen, G., Halberg, F., Takeshima, T., Kaplan, D. T., … Shimizu, E. (2005). Approximate entropy in the electroencephalogram during wake and sleep. *Clinical EEG and Neuroscience*, *36*, 21–24.

Carhart-Harris, R. L., Leech, R., Hellyer, P. J., Shanahan, M., Feilding, A., Tagliazucchi, E., …, Nutt, D. 2014. The entropic brain: A theory of conscious states informed by neuroimaging research with psychedelic drugs. *Frontiers in Human Neuroscience 8*, 20.

Carhart-Harris, R. L. (2018). The entropic brain - revisited. *Neuropharmacology*, in press.

Castiglioni, P., Coruzzi, P., Bini, M., Parati, G., & Faini, A. (2017). Multiscale sample entropy of cardiovascular signals: Does the choice between fixed-or varying-tolerance among scales influence its evaluation and interpretation? *Entropy*, *19*, 590.

Celada, P., Puig, M. V., & Artigas, F. (2013). Serotonin modulation of cortical neurons and networks. *Frontiers in Integrative Neuroscience*, *7*, 25.

Concas, A., Santoro, G., Serra, M., Sanna, E., & Biggio, G. (1991). Neurochemical action of the general anaesthetic propofol on the chloride ion channel coupled with GABAA receptors. *Brain Research*, *542*, 225–232.

Costa, M., Goldberger, A. L., & Peng, C. K. (2002). Multiscale entropy analysis of complex physiologic time series. *Physical Review Letters*, *89*, 068102.

Costa, M., Goldberger, A. L., & Peng, C. K. (2005). Multiscale entropy analysis of biological signals. *Physical Review E, Statistical, Nonlinear, and Soft Matter Physics*, *71*(2 Pt 1), 021906.

Cote, K. A. (2002). Probing awareness during sleep with the auditory odd-ball paradigm. *International Journal of Psychophysiology*, *46*, 227–241.

Cote, K. A., Etienne, L., & Campbell, K. B. (2001). Neurophysiological evidence for the detection of external stimuli during sleep. *Sleep*, *24*, 791–803.

Courtiol, J., Perdikis, D., Petkoski, S., Müller, V., Huys, R., Sleimen-Malkoun, R., & Jirsa, V. K. (2016). The multiscale entropy: Guidelines for use and interpretation in brain signal analysis. *Journal of Neuroscience Methods*, *273*, 175–190.

Dash, M. B., Douglas, C. L., Vyazovskiy, V. V., Cirelli, C., & Tononi, G. (2009). Long-term homeostasis of extracellular glutamate in the rat cerebral cortex across sleep and waking states. *The Journal of Neuroscience*, *29*, 620–629.

Deco, G., Jirsa, V. K., & McIntosh, A. R. (2011). Emerging concepts for the dynamical organization of resting-state activity in the brain. *Nature Reviews. Neuroscience*, *12*, 43–56.

Deghani, N., Bédard, C., Cash, S. S., Halgren, E., & Destexhe, A. (2010). Comparative power spectral analysis of simultaneous electroencephalographic and magnetoencephalographic recordings in humans suggest non-resistive extracellular media. *Journal of Computational Neuroscience*, *29*, 405–421.

Delorme, A., & Makeig, S. (2004). EEGLAB: An open source toolbox for analysis of single-trial EEG dynamics including independent component analysis. *Journal of Neuroscience Methods*, *134*, 9–21.

Ferenets, R., Vanluchene, A., Lipping, T., Heyse, B., & Struys, M. M. (2007). Behavior of entropy/complexity measures of the electroencephalogram during propofol-induced sedation: Dose-dependent effects of remifentanil. *Anesthesiology*, *106*, 696–706.

Fransson, P., Metsäranta, M., Blennow, M., Åden, U., Lagercrantz, H., & Vanhatalo, S. (2013). Early development of spatial patterns of power-law frequency scaling in FMRI resting-state and EEG data in the newborn brain. *Cerebral Cortex*, *23*, 638–646.

Freeman, W. J., Holmes, M. D., Burke, B. C., & Vanhatalo, S. (2003). Spatial spectra of scalp EEG and EMG from awake humans. *Clinical Neurophysiology*, *114*, 1053–1068.

Freeman, W. J., & Zhai, J. (2009). Simulated power spectral density (PSD) of background electrocorticogram (ECoG). *Cognitive Neurodynamics*, *3*, 97–103.

Gao, R. (2016). Interpreting the electrophysiological power spectrum. *Journal of Neurophysiology*, *115*, 628–630.

Gao, R., Peterson, E. J., & Voytek, B. (2017). Inferring synaptic excitation/inhibition balance from field potentials. *NeuroImage*, *158*, 70–78.

Garrett, D. D., Samanez-Larkin, G. R., MacDonald, S. W., Lindenberger, U., McIntosh, A. R., & Grady, C. L. (2013). Moment-to-moment brain signal variability: A next frontier in human brain mapping? *Neuroscience and Biobehavioral Reviews*, *37*, 610–624.

Goldberger, A. L., Peng, C. K., & Lipsitz, L. A. (2002). What is physiologic complexity and how does it change with aging and disease? *Neurobiology of Aging*, *23*, 23–26.

Groppe, D. M., Urbach, T. P., & Kutas, M. (2011). Mass univariate analysis of event-related brain potentials/fields I: A critical tutorial review. *Psychophysiology*, *48*, 1711–1725.

Hansen, E. C., Battaglia, D., Spiegler, A., Deco, G., & Jirsa, V. K. (2015). Functional connectivity dynamics: Modeling the switching behavior of the resting state. *NeuroImage*, *105*, 525–535.

He, B. J. (2014). Scale-free brain activity: Past, present, and future. *Trends in Cognitive Sciences*, *18*, 480–487.

He, X., Koo, B. B., & Killiany, R. J. (2016). Edited magnetic resonance spectroscopy detects an age-related decline in nonhuman primate brain GABA levels. *BioMed Research International*, *2016*, 1, 6523909–7.

He, B. J., Zempel, J. M., Snyder, A. Z., & Raichle, M. E. (2010). The temporal structures and functional significance of scale-free brain activity. *Neuron*, *66*, 353–369.

Heisz, J. J., Gould, M., & McIntosh, A. R. (2015). Age-related shift in neural complexity related to task performance and physical activity. *Journal of Cognitive Neuroscience*, *27*, 605–613.

Kaffashi, F., Foglyano, R., Wilson, C. G., & Loparo, K. A. (2008). The effect of time delay on approximate & sample entropy calculations. *Physica D*, *237*, 3069–3074.

Kuntzelman, K., Rhodes, L. J., Harrington, L. N., & Miskovic, V. (2018). A practical comparison of algorithms for the measurement of multiscale entropy of neural time series data. *Brain and Cognition*, *123*, 126–135.

Lee, G. M., Fattinger, S., Mouthon, A. L., Noirhomme, Q., & Huber, R. (2013). Electroencephalogram approximate entropy influenced by both age and sleep. *Frontiers in Neuroinformatics*, *7*, 33.

Llinás, R. R., & Paré, D. (1991). Of dreaming and wakefulness. *Neuroscience*, *44*, 521–535.

Lombardi, F., Herrmann, H. J., & de Arcangelis, L. (2017). Balance of excitation and inhibition determines 1/f power spectrum in neuronal networks. *Chaos*, *27*, 047402.

Ma, Y., Shi, W., Peng, C. K., & Yang, A. C. (2017). Nonlinear dynamical analysis of sleep electroencephalography using fractal and entropy approaches. *Sleep Medicine Reviews*, *37*, 85–93.

MacDonald, K. J., & Cote, K. A. (2016). Sleep physiology predicts memory retention after reactivation. *Journal of Sleep Research*, *25*, 655–663.

Manning, J. R., Jacobs, J., Fried, I., & Kahana, M. J. (2009). Broadband shifts in local field potential power spectra are correlated with single-neuron spiking in humans. *The Journal of Neuroscience*, *29*, 13613–13620.

Massimi, M., Ferrarelli, F., Huber, R., Esser, S. K., Singh, H., & Tononi, G. (2005). Breakdown of cortical effective connectivity during sleep. *Science*, *309*, 2228–2232.

Mateos, D. M., Guevara Erra, R., Wennberg, R., & Perez Velazquez, J. L. (2018). Measures of entropy and complexity in altered states of consciousness. *Cognitive Neurodynamics*, *12*, 73–84.

McDonough, I. M., & Nashiro, K. (2014). Network complexity as a measure of information processing across resting-state networks: Evidence from the human connectome project. *Frontiers in Human Neuroscience*, *8*, 409.

McIntosh, A. R., Vakorin, V., Kovacevic, N., Wang, H., Diaconescu, A., & Protzner, A. B. (2014). Spatiotemporal dependency of age-related changes in brain signal variability. *Cerebral Cortex*, *24*, 1806–1817.

Miller, K. J., Honey, C. J., Hermes, D., Rao, R. P., denNijs, M., & Ojemann, J. G. (2014). Broadband changes in the cortical surface potential track activation of functionally diverse neuronal populations. *NeuroImage*, *85*(Pt 2), 711–720.

Mizuno, T., Takahashi, T., Cho, R. Y., Kikuchi, M., Murata, T., Takahashi, K., & Wada, Y. (2010). Assessment of EEG dynamical complexity in Alzheimer's disease using multiscale entropy. *Clinical Neurophysiology*, *121*, 1438–1446.

Muthukumaraswamy, S. D., Carhart-Harris, R. . L., Moran, R. J., Brookes, M. J., Williams, T. M., Errtizoe, D., … Nutt, D. J. (2013). Broadband cortical desynchronization underlies the human psychedelic state. *The Journal of Neuroscience*, *33*, 15171–15183.

Nayak, C. S., Bhowmik, A., Prasad, P. D., Pati, S., Choudhury, K. C., & Majumdar, K. K. (2017). Phase synchronization analysis of natural wake and sleep states in healthy individuals using a novel ensemble phase synchronization measure. *Journal of Clinical Neurophysiology*, *34*, 77–83.

Nicolaou, N., & Georgiou, J. (2011). The use of permutation entropy to characterize sleep electroencephalograms. *Clinical EEG and Neuroscience*, *42*, 24–28.

Park, J.-H., Kim, S., Kim, C.-H., & Cichocki, A. (2007). Multiscale entropy analysis of EEG from patients under different pathological conditions. *Fractals*, *15*, 399–404.

Pedersen, M., Omidvarnia, A., Walz, J. M., Zalesky, A., & Jackson, G. D. (2017). Spontaneous brain network activity: Analysis of its temporal complexity. *Network Neuroscience*, *1*, 100–115.

Peng, C. K., Costa, M., & Goldberger, A. L. (2009). Adaptive data analysis of complex fluctuations in physiologic time series. *Advances in Adaptive Data Analysis*, *1*, 61–70.

Pereda, E., Gamundi, A., Rial, R., & González, J. (1998). Non-linear behaviour of human EEG: Fractal exponent versus correlation dimension in awake and sleep stages. *Neuroscience Letters*, *250*, 91–94.

Pincus, S. M., & Goldberger, A. L. (1994). Physiological time-series analysis: What does regularity quantify? *The American Journal of Physiology*, *266*, H1643–H1656.

Pivik, R. T. (2007). Sleep and dreaming. In J. T. Cacioppo, L. G. Tassinary, & G. G. Berntson (Eds.), *Handbook of psychophysiology* (pp. 633–662). New York, NY: Cambridge University Press.

Podvalny, E., Noy, N., Harel, M., Bickel, S., Chechik, G., Schroeder, C. E., … Malach, R. (2015). A unifying principle underlying the extracellular field potential spectral responses in the human cortex. *Journal of Neurophysiology*, *114*, 505–519.

Porges, E. C., Woods, A. J., Edden, R. A., Puts, N. A., Harris, A. D., Chen, H., … Cohen, R. A. (2017). Frontal gamma-aminobutyric acid concentrations are associated with cognitive performance in older adults. *Biological Psychiatry: Cognitive Neuroscience and Neuroimaging*, *2*, 38–44.

Pozzorini, C., Naud, R., Mensi, S., & Gerstner, W. (2013). Temporal whitening by power-law adaptation in cortical neurons. *Nature Neuroscience*, *16*, 942–948.

Pritchard, W. S. (1992). The brain in fractal time: 1/f-like power spectrum scaling of the human electroencephalogram. *The International Journal of Neuroscience*, *66*, 119–129.

R Development Core Team, 2008. R: A language and environment for statistical computing. Retrieved from http://www.r-project.org

Rechtshaffen, A., & Kales, A. A. (1968). *A manual of standardized terminology, techniques and scoring system for sleep stages of human subjects*. Bethesda, MD: US National Institute of Neurological Diseases and Blindness.

Rostaghi, M., & Azami, H. (2016). Dispersion entropy: A measure for time-series analysis. *IEEE Signal Processing Letters*, *23*, 610–614.

Sanchez-Vives, M. V., & McCormick, D. A. (2000). Cellular and network mechanisms of rhythmic recurrent activity in neocortex. *Nature Neuroscience*, *3*, 1027–1034.

Schartner, M. M., Carhart-Harris, R. L., Barrett, A. B., & Seth, A. K. (2017). Increased spontaneous MEG signal diversity for psychoactive doses of ketamine, LSD and psilocybin. *Scientific Reports*, *7*, 46421.

Schartner, M. M., Pigorini, A., Gibbs, S. A., Arnulfo, G., Sarasso, S., Barnett, L., … Barrett, A. B. (2017). Global and local complexity of intracranial EEG decreases during NREM sleep. *Neuroscience of Consciousness*, *1*, niw022.

Schartner, M. M., Seth, A., Noirhomme, Q., Boly, M., Bruno, M. A., Laureys, S., & Barrett, A. (2015). Complexity of multi-dimensional spontaneous EEG decreases during propofol induced general anesthesia. *PLoS One*, *10*, e0133532.

Schreiber, T., & Schmitz, A. (1996). Improved surrogate data for nonlinearity tests. *Physical Review Letters*, *77*, 635–638.

Schwartz, J. R., & Roth, T. (2008). Neurophysiology of sleep and wakefulness: Basic science and clinical implications. *Current Neuropharmacology*, *6*, 367–378.

Sejdić, E., & Lipsitz, L. A. (2013). Necessity of noise in physiology and medicine. *Computer Methods and Programs in Biomedicine*, *111*, 459–470.

Sheehan, T. C., Sreekumar, V., Inati, S. K., & Zaghloul, K. A. (2018). Signal complexity of human intracranial EEG tracks successful associative-memory formation across individuals. *The Journal of Neuroscience*, *38*, 1744–1755.

Shen, Y., Olbrich, E., Achermann, P., & Meier, P. F. (2003). Dimensional complexity and spectral properties of the human sleep EEG. *Clinical Neurophysiology*, *114*, 199–209.

Shi, W., Shang, P., Ma, Y., Sun, S., & Yeh, C.-H. (2017). A comparison study on stages of sleep: Quantifying multiscale complexity using higher moments on coarse-graining. *Communications in Nonlinear Science and Numerical Simulation*, *44*, 292–303.

Spoormaker, V. I., Schröter, M. S., Gleiser, P. M., Andrade, K. C., Dresler, M., Wehrle, R., … Czisch, M. (2010). Development of a large-scale functional brain network during human non-rapid eye movement sleep. *The Journal of Neuroscience*, *20*, 11379–11387.

Steriade, M., Timofeev, I., & Grenier, F. (2001). Natural waking and sleep states: A view from inside neocortical neurons. *Journal of Neurophysiology*, *85*, 1969–1985.

Supp, G. G., Siegel, M., Hipp, J. F., & Engel, A. K. (2011). Cortical hypersynchrony predicts breakdown of sensory processing during loss of consciousness. *Current Biology*, *21*, 1988–1993.

Tagliazucchi, E. (2017). The signatures of conscious access and its phenomenology are consistent with large-scale brain communication at criticality. *Consciousness and Cognition*, *55*, 136–147.

Tagliazucchi, E., Behrens, M., & Laufs, O. (2013). Sleep neuroimaging and models of consciousness. *Frontiers in Psychology*, *4*, 256.

Tagliazucchi, E., Carhart-Harris, R., Leech, R., Nutt, D., & Chialvo, D. R. (2014). Enhanced repertoire of brain dynamical states during the psychedelic experience. *Human Brain Mapping*, *35*, 5442–5456.

Tagliazucchi, E., von Wegner, F., Morzelewski, A., Brodbeck, V., Borisov, V., Jahnke, K., & Laufs, H. (2013). Large-scale brain functional modularity is reflected in slow electroencephalographic rhythms across the human non-rapid eye movement sleep cycle. *NeuroImage*, *70*, 327–339.

Theiler, J., Eubank, S., Longtin, A., Galdrikian, B., & Farmer, J. D. (1992). Testing for nonlinearity in time series: The method of surrogate data. *Physica D*, *58*, 77–94.

Tononi, G., & Koch, C. (2008). The neural correlates of consciousness: An update. *Annals of the New York Academy of Sciences*, *1124*, 239–261.

Tröbs, M., & Heinzel, G. (2006). Improved spectrum estimation from digitized time series on a logarithmic frequency axis. *Measurement*, *39*, 120–129.

Vakorin, V. A., Lippé, S., & McIntosh, A. R. (2011). Variability of brain signals processed locally transforms into higher connectivity with brain development. *The Journal of Neuroscience*, *31*, 6405–6413.

Vakorin, V. A., & McIntosh, A. R. (2012). Mapping the multi-scale information content of complex brain signals. In M. Rabinovich, K. Friston, & P. Varona (Eds.), *Principles of brain dynamics: Global state interactions* (pp. 183–208). Cambridge, MA: The MIT Press.

Viol, A., Palhano-Fontes, F., Onias, H., de Araujo, D. B., & Viswanathan, G. M. (2017). Shannon entropy of brain functional complex networks under the influence of psychedelic Ayahuasca. *Scientific Reports*, *7*, 7388.

Volk, C., Jaramillo, V., Merki, R., O'Gorman Tuura, R., & Huber, R. (in press). Diurnal changes in glutamate + glutamine levels of healthy young adults assessed by proton magnetic resonance spectroscopy. *Human Brain Mapping*.

Voytek, B., & Knight, R. T. (2015). Dynamic network communication as a unifying neural basis for cognition, development, aging, and disease. *Biological Psychiatry*, *77*, 1089–1097.

Voytek, B., Kramer, M. A., Case, J., Lepage, K. Q., Tempesta, Z. R., Knight, R. T., & Gazzaley, A. (2015). Age-related changes in 1/f neural electrophysiological noise. *The Journal of Neuroscience*, *35*, 13257–13265.

Vyazovskiy, V. V., Cirelli, C., Pfister-Genskow, M., Faraguna, U., & Tononi, G. (2008). Molecular and electrophysiological evidence for net synaptic potentiation in wake and depression in sleep. *Nature Neuroscience*, *11*, 200–208.

Wang, H., McIntosh, A. R., Kovacevic, N., Karachalios, M., & Protzner, A. B. (2016). Age-related multiscale changes in brain signal variability in pre-task versus post-task resting-state EEG. *Journal of Cognitive Neuroscience*, *28*, 971–984.

Waschke, L., Wöstmann, M., & Obleser, J. (2017). States and traits of neural irregularity in the age-varying human brain. *Scientific Reports*, *7*, 17381.

Wen, H., & Liu, Z. (2016). Separating fractal and oscillatory components in the power spectrum of neurophysiological signal. *Brain Topography*, *29*, 13–26.

Zhang, X.-S., Roy, R. J., & Jensen, E. W. (2001). EEG complexity as a measure of depth of anesthesia for patients. *IEEE Transactions on Biomedical Engineering*, *48*, 1424–1433.

SUPPORTING INFORMATION

Additional supporting information may be found online in the Supporting Information section at the end of the article.

How to cite this article: Miskovic V, MacDonald KJ, Rhodes LJ, Cote KA. Changes in EEG multiscale entropy and power-law frequency scaling during the human sleep cycle. *Hum Brain Mapp*. 2019;40:538–551. https://doi.org/10.1002/hbm.24393